Photoreactivity in Self-Assembled Monolayers Formed from Asymmetric Disulfides Having para-Substituted Azobenzenes

Haruhisa Akiyama,* Kaoru Tamada,* Jun'ichi Nagasawa, Koji Abe, and Takashi Tamaki

National Institute of Advanced Industrial Science and Technology (AIST), Central 5, 1-1-1 Higashi, Tsukuba, Ibaraki 305-8565, Japan

Received: May 13, 2002; In Final Form: October 27, 2002

Asymmetric dialkyl disulfides with a para-substituted azobenzene (i.e., 4-substituted 4′-(12-(dodecyldithio)-dodecyloxy)azobenzenes) produced photoresponsive self-assembled monolayers (SAMs) on gold (111) surfaces. Infrared reflection absorption (IR-RA) spectroscopy and reflection ultraviolet (UV) and visible (vis) light absorption spectroscopy gave information on the molecular orientational order of the adsorbates in the SAMs. The photoreactivity was investigated using dynamic contact-angle measurements with a Wilhelmy-type surface balance. The structure and photoreactivity of the SAMs were dependent on the substituent at the para position of an azobenzene moiety. Relatively ordered structures in the methylene parts and the photoisomerization of azobenzene moieties were observed for the SAMs formed from the hexyl- and the nonsubstituted azobenzene disulfides. However, a less-ordered SAM structure was seen for the cyanoazobenzene disulfide SAM, and the photoresponse is rather unstable.

1. Introduction

It is known that the self-assembling of long alkanethiols and alkyl disulfides on a gold (111) surface produces a well-ordered monolayer.[1] One of its prominent characteristics is the ease of preparing various types of functional monolayer surfaces, which can be achieved by using terminal-substituted alkanethiols with different kinds of functional groups.[2] Recently, the introduction of an azobenzene dye into SAMs has been attempted, resulting in unique SAM structures.[3] Since azobenzene is photoisomerizable from trans to cis isomers and from cis to trans isomers upon irradiation with UV light (365 nm) and with vis light (436 nm), respectively, such SAMs could have the potential for photoresponse. However, the introduction of an azobenzene chromophore into the alkanethiol terminal could not produce a photoisomerizable monolayer because there was not enough space to photoisomerize in well-packed molecular films. For instance, Wang et al. actually clarified that the azobenzene moieties in a SAM composed of azobenzene-terminated alkanethiols gave only a 5% or less yield of the cis isomer upon irradiation with ultraviolet light.[4] This means that a sweep volume[5] is necessary for the isomerization of azobenzenes, even in a monolayer. Therefore, the regulation of the 2D density of the chromophores is important for the formation of a photoresponsive monolayer. There have been other photoresponsive monolayers composed of azobenzene derivatives by various methods such as the Langmuir−Blodgett (LB) technique,[6] a silano-coupling self-assembling method,[7] and so on. Among them, the relation between the photoreactivity and the occupied area of an azobenzene moiety has been reported for monolayers that are composed of azobenzene macrocyclic amphiphilic adsorbates and stabilized by multisite hydrogen bonding or ionic interaction on the substrates.[8,9] Their results indicate that the critical area required for the isomerization of alkylazobenzenes is 45 Å^2/molecule.[9] For long-chain 1-alkanethiol SAMs on gold (111), a $(\sqrt{3} \times \sqrt{3})R30°$ hexagonal lattice has been observed as one of the most stable overlayer structures, indicating that the sulfur atoms bind to a specific site on the gold lattice.[10] In this case, each adsorbate definitely occupies an area of 21.7 Å^2/molecule, which is almost half of the critical area for azobenzene isomerization. Evans et al. used a SAM formed from a mixture of alkanethiol and azobenzene-terminated alkanethiol to dilute azobenzene moieties and maintain the photoreactivity.[11] However, it is generally difficult to control the composition ratio and to achieve a molecular dispersity in such a mixed SAM because phase separation and preferential adsorption take place during SAM formation.[12] Although the phase separation in asymmetric disulfide SAMs has also been observed in a low-molecular-density film[13] or after annealing at high temperature,[14] an asymmetric disulfide has been reported to give a 1:1 mixed SAM with a reduced phase segregation.[15] Therefore, we prepared asymmetric disulfides with an alkyl group on one side and an azobenzene-terminated alkyl group on the other side to avoid phase separation and to dilute the azobenzene moieties by half. A definite photoresponse of the SAMs formed from these asymmetric disulfides on gold has been observed on the basis of the measurements of static contact angles[16] and surface plasmon resonance spectroscopy.[17] It is of great interest to confirm whether the azobenzene tail groups at the para position in the outermost position of the monolayer affect the photoreactivity because the sweep volume for isomerization will be changed depending on their size and on monolayer structures because of the difference in the lateral interaction during monolayer formation. In this study, we prepare SAMs with three kinds of azobenzene-containing asymmetric disulfides, which have hexyl, cyano, or no functional groups as a tail group at the *p*′ position of 4-(12-(dodecyldithio)dodecyloxy)azobenzene, to investigate the substituent effects on the structures and photoreactivity using dynamic contact-angle measurement, IR-RA spectroscopy, and reflection absorption spectroscopy.

* To whom correspondence should be addressed. E-mail: h.akiyama@aist.go.jp. Tel: +81-298-61-4672. Fax: +81-298-61-4673. E-mail: k-tamada@aist.go.jp. Tel: +81-298-61-6305. Fax: +81-298-61-6303.

10.1021/jp026103g CCC: $25.00
Published on Web 12/04/2002

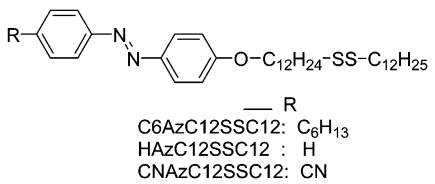

Figure 1. Structure of asymmetric disulfides.

2. Experimental Section

Materials. The 4-substituted 4′-(12-(dodecyldithio)dodecyloxy)azobenzenes shown in Figure 1 were prepared from the corresponding 4-hydroxyazobenzene derivatives. The reaction of the 4-substituted 4′-hydroxyazobenzenes with dibromododecane yielded 4-substituted 4′-(12-bromododecyloxy)azobenzenes, and they were converted to a Bunte salt by reaction with sodium thiosulfate. The Bunte salt was reacted with 1-dodecanethiolate to produce the azobenzene disulfides. The detailed synthesis method of one of these compounds, 4-hexyl-4′-(12-(dodecyldithio)dodecyloxy)azobenzenes, has been reported elsewhere,[16] and the other compounds were synthesized using a similar method. The analytical data of all of the compounds are listed here for identification only.

4-Hexyl-4′-(12-(dodecyldithio)dodecyloxy)azobenzene (C6AzSSC12). Mp: 68.5−69.5 °C. ^{1}H NMR ($CDCl_3$, δ): 0.88 (3H, t, $-CH_3$), 0.89 (3H, t, $-CH_3$), 1.4−1.6 (40H, m, $CH_2-CH_2-CH_2$), 1.65 (4H, t, t, $S-S-CH_2-CH_2$), 1.67 (2H, t, t, $Ar-CH_2-CH_2$), 1.82 (2H, t, t, $Ar-O-CH_2-CH_2$), 2.68 (2H, t, $Ar-CH_2$), 2.68 (4H, t, $S-S-CH_2$), 4.03 (2H, t, $Ar-O-CH_2$), 6.99 (2H, d, Ar−H), 7.29 (2H, d, Ar−H), 7.79 (2H, d, Ar−H), 7.89 (2H, d, Ar−H). Elemental Analysis Calcd (wt %): C, 73.84; H, 10.33; N, 4.10; S, 9.39. Found (wt %): C, 73.80; H, 10.44; N, 4.12; S, 9.37.

4-Cyano-4′-(12-(dodecyldithio)dodecyloxy)azobenzene (CNAzSSC12). Mp: 75−76 °C. T_c (clearing temperature: this compound showed a liquid crystalline phase) 81 °C. ^{1}H NMR ($CDCl_3$, δ): 0.88 (3H, t, $-CH_3$), 1.2−1.6 (34H, m, $CH_2-CH_2-CH_2$), 1.67 (4H, t, t, $S-S-CH_2-CH_2$), 1.83 (2H, t, t, $Ar-O-CH_2-CH_2$), 2.68 (4H, t, $S-S-CH_2$), 4.01 (2H, t, $Ar-O-CH_2$), 7.02 (2H, d, Ar−H), 7.79 (2H, d, Ar−H), 7.94 (4H, d, Ar−H). Elemental Analysis Calcd (wt %): C, 71.22; H, 9.21 N, 6.73; S, 10.28. Found (wt %): C, 71.48; H, 9.46; N, 6.71; S, 10.37.

4-(12-(Dodecyldithio)dodecyloxy)azobenzene (HAzSSC12). Mp: 77.0−78.5 °C. ^{1}H NMR ($CDCl_3$, δ): 0.88 (3H, t, $-CH_3$), 1.2−1.6 (34H, m, $CH_2-CH_2-CH_2$), 1.67 (4H, t, t, $S-S-CH_2-CH_2$), 1.82 (2H, t, t, $Ar-O-CH_2-CH_2$), 2.68 (4H, t, $S-S-CH_2$), 4.04 (2H, t, $Ar-O-CH_2$), 7.01 (2H, d, Ar−H), 7.43 (1H, t, Ar−H), 7.50 (2H, t, Ar−H), 7.87 (2H, d, Ar−H), 7.91 (2H, d, Ar−H). Elemental Analysis Calcd (wt %): C, 72.19; H, 9.76; N, 4.68; S, 10.71. Found (wt %): C, 72.43; H, 9.81; N, 4.73; S, 10.73.

SAM Preparation. Gold was thermally deposited on cleaved mica plates (1 cm × 2 cm) in a vacuum chamber in which the pressure was kept at (2.5−3.0) × 10^{-7} Torr during the gold evaporation at 430 °C. After the deposition of a layer that was 1000−2000 Å in thickness, the gold-layered substrates were annealed at 570 °C for 2 h. The substrates with a gold thickness of 1000−1500 Å were used for the contact-angle measurements and reflection absorption spectroscopy, and those of 1500−2000 Å thickness, for IR spectroscopy.

The freshly prepared gold-layered substrates were immediately put into 10^{-4} mol/dm^3 dichloromethane solutions containing the disulfide compounds. These substrates were rinsed several times with pure dichloromethane to eliminate the free disulfides and were then dried under air.

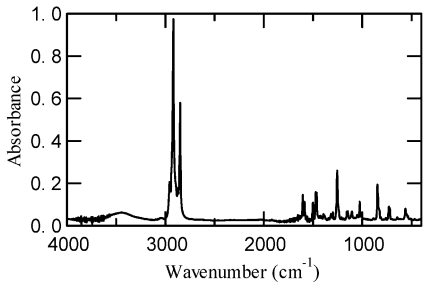

Figure 2. IR spectrum of C6AzSSC12 powders in a KBr pellet.

Infrared Reflection Absorption (IR-RA) Spectroscopy. The IR-RA spectra were measured at 4 cm^{-1} resolution with a p-polarized monitoring beam on a Perkin-Elmer system 2000 FT-IR spectrometer equipped with an MCT detector, where the incident angle of the p-polarized infrared light was set at 80° against the normal direction to the sample plane. The background compensation was carried out by the subtraction of the spectrum of a perdeuterated 1-dodecanelthiol-d25 SAM from the sample spectra.

Dynamic Contact-Angle (DCA) Measurement. Dynamic contact-angle (DCA) measurements were conducted using the Wilhelmy plate method with a Cahn balance (DCA 322 model) using deionized and distilled water in which the moving rate of the sample was 20 μm/s. We used a modified technique to measure the asymmetric Au−thiol SAM plate (Au−thiol SAMs on one side and naked mica on the other side). In this method, the contact angle of the SAM surface was estimated by a simple numerical calculation from the force F acting on the sample plate, where perfect wetting ($\theta = 0°$) of the freshly cleaved mica surface was assumed. The details of this technique are presented in the literature.[18] Since surface roughness can have an impact on the hysteresis in contact angles,[19] gold films were deposited under the same conditions for all of the experiments.

Reflection UV−Vis Absorption Spectroscopy. The UV−vis absorption spectra of the solution and films were obtained using a Shimadzu UV-2500PC spectrometer. The asymmetric disulfides were dissolved in hexane at a concentration of 2.0 × 10^{-5} mol/dm^3 for the measurements. For the reflection measurements of the films, a mirror unit for reflection spectroscopy was attached to the spectrometer at 5° to the incident angle of the probe light against the sample plane. A bare gold-deposited mica plate was used here as a reference. Photoirradiation of the sample was carried out with an ultra-high-pressure 500-W mercury arc (Ushio) with a combination of color filters: ZwB2 and WB360 (Optima) for 365-nm light of ca. 20 mW/cm^2 and Y-44 and B-460 (Hoya) for 436-nm light.

Calculations of the Dipole Moments of the Model Compounds. Calculations of the dipole moments were made with the MM and AM1 methods using Win-MOPAC (Fujitsu). 4-Butoxy-4′-hexylazobenzene and 4-butoxy-4′-cyanoazobenzene were used the model compounds for C6AzSSC12 and CNAzSSC12, respectively.

3. Results and Discussion

3.1. IR-RA Spectroscopy. Figures 2 and 3 show the IR spectrum of C6AzSSC12 powder in a KBr pellet and the IR-RA spectra of SAMs prepared by the immersion of substrates into a sample solution for 10 min, 1 h, 24 h, and 3 days, respectively. Absorption peaks at 1605, 1587, 1501, 1473, and 1463 cm^{-1} in the bulk sample shown in Figure 2 are assigned to benzene ring stretchings whereas the peak at 1255 cm^{-1} corresponds to C−O−C stretching.[3a,20] Similar peaks are

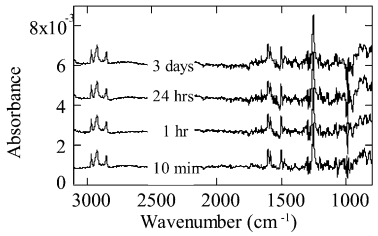

Figure 3. IR-RA spectra of C6AzSSC12 SAMs on gold (111) prepared by the immersion of a substrate into the sample solution for 10 min, 1 h, 24 h, and 3 days.

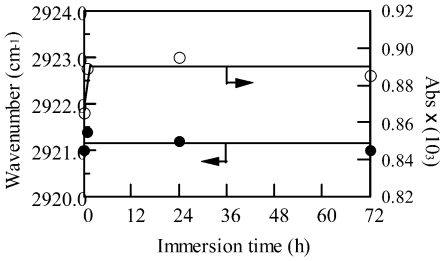

Figure 4. Position (●) and intensity (○) of IR peaks corresponding to $\nu_{as}(CH_2)$ bands in C6AzSSC12 SAMs versus immersion time.

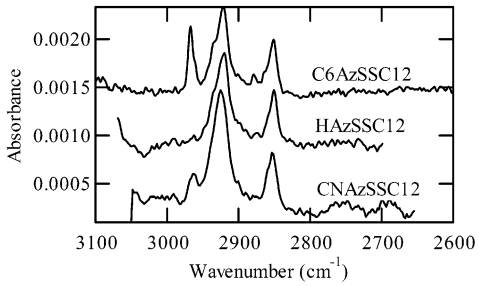

Figure 5. IR-RA spectra of asymmetric disulfide SAMs in the region from 2600 to 3100 cm^{-1}.

observed at 1603, 1585, 1501, 1476, and 1253 cm^{-1} in Figure 3, proving the presence of azobenzene moieties in the SAMs. The peaks attributed to $\nu_{as}(CH_3)$, $\nu_{as}(CH_2)$, and $\nu_s(CH_2)$ are observed at around 2967, 2921, and 2851 cm^{-1} in the spectra of the SAMs.[21] It is known that the frequencies of the methylene stretching bands are sensitive to the conformation of the alkyl chain; the values of 2921 and 2851 cm^{-1} observed here correspond to a trans zigzag conformation of methylenes that includes a small portion of the gauche structure.[22]

In the spectra of four different immersion times in Figure 3, there were no significant differences in the strength and intensity ratio of each peak. For the sake of comparison, the position and height at the peak top versus the incubation time are plotted in Figure 4. Samples prepared by immersion for more than 1 h show similar values under our experimental conditions, indicating that the 1-h immersion time is long enough to complete the adsorption. Moreover, no features showing phase separation and decomposition appeared during the 3-day immersion in these spectra. The IR-RA spectra of the HAzSSC12 and CNAzSSC12 SAMs prepared by a 1-h immersion are shown in Figure 5 together with that of C6AzSSC12. The peaks of the methylene stretching appear at similar positions to those of C6AzSSC12, indicating the relatively ordered structure of an alkyl chain. A clearly different feature from the C6AzC12SSC12 SAM spectrum is that HAzSSC12 has no peaks corresponding to the asymmetric stretching vibration of the methyl C−H ($\nu_{as}(CH_3)$). When the direction of a methyl asymmetric vibration at the terminal CH_3 is almost parallel to the substrate plane, a C−H ($\nu_{as}(CH_3)$) peak disappears because of the orthogonal orientation

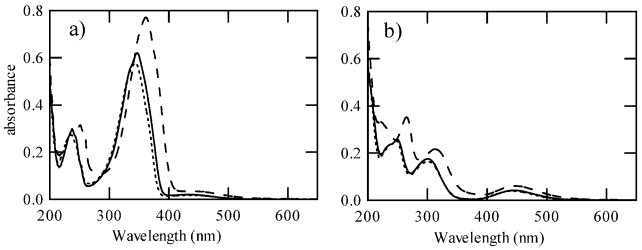

Figure 6. Absorption spectra of HAzSSC12 (· ·), C6AzSSC12 (—), and CNAzSSC12 (− −) in hexane solutions (a) before and (b) after irradiation with UV light.

TABLE 1: Wavenumbers and Absorbances of $\nu_{as}(CH_2)$ Bands for Asymmetric Disulfide SAMs

	C6AzC12SSC12	HAzC12SSC12	CNAzC12SSC12
wavenumber (cm^{-1})	2921	2920	2924
absorbance	0.0009	0.0008	0.0013

to the electric vibration of the monitoring IR light under the RAS condition, as reported for a 1-octadecanethiol SAM on a large-grain gold substrate in our previous study.[3a] It is quite possible for the dodecylthiorate parts in a HAzSSC12 SAM to take on a conformation similar to that of 1-octadecanethiol because both molecules have a relatively large odd number of carbons.[23] From this viewpoint, a C−H ($\nu_{as}(CH_3)$) peak from the methyl group of the dodecyl part in a C6AzSSC12 SAM probably disappears or similarly weakens. Therefore, the strong C−H ($\nu_{as}(CH_3)$) peak that appeared in the IR-RA spectra of the C6AzSSC12 SAM can be attributed to the absorption of the terminal CH_3 of a hexyl substituent at the para position of the azobenzene. However, the IR spectrum of CNAzSSC12 shows weak absorption bands corresponding to C−H ($\nu_{as}(CH_3)$), though it has no alkyl substituent at the azobenzene tails. It should be ascribed to the terminal CH_3 of the dodecyl parts, suggesting a less-ordered chain conformation in contrast to that for HAzSSC12. This is supported by the higher wavenumber (2924 cm^{-1}) position of the methylene absorption peak compared to those of HAzSSC12 and C6AzSSC12 (2920 and 2921 cm^{-1}), as shown in the Table 1. In the case of CNAzSSC12, the peak position was unchanged for a 3-day immersion sample whereas the peak intensity is a little higher than that of the 1-h immersion sample (i.e., the adsorption process of CNAzSSC12 might be a little slower than the other two). It is likely that CNAzSSC12 does not form a crystallinelike SAM even after a 3-day immersion. Therefore, SAMs prepared by the 1-h immersion in each solution were used in the following experiments to be compared under a unified condition.

3.2. UV Reflection Spectra. Figure 6a and b show the UV absorption spectra of three kinds of azobenzenes containing disulfides in hexane before and after irradiation with UV light. The peak positions of λ_{max} before irradiation are 344 nm for HAzSSC12, 347 nm for C6AzSSC12, and 361 nm for CNAzSSC12, corresponding to the $\pi-\pi^*$ absorption of the trans isomers. The molar extinction coefficients (ϵ) at λ_{max} increase in this order: 2.8×10^4, 3.1×10^4, and 3.8×10^4 mol^{-1} dm^3 cm^{-1}. Substituents of chromophores can cause the peak to shift and enlarge because they work as auxochromes. After irradiation, a characteristic absorption band around 350 nm disappeared, and a weaker $\pi-\pi^*$ band corresponding to a cis isomer appeared at around 300 nm.

Figure 7 shows the reflection UV−vis absorption spectra of the C6AzSSC12, HAzSSC12, and CNAzSSC12 SAMs. They are different from those in solution. The transition moment for the characteristic $\pi-\pi^*$ absorption band around 350 nm of the trans isomers is almost parallel to the molecular axis.[24] By

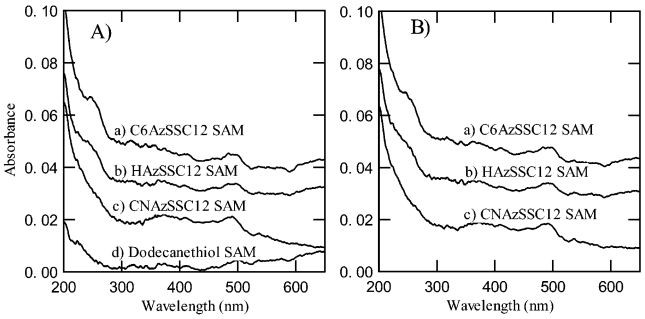

Figure 7. UV−vis reflection spectra of (a) C6AzSSC12, (b) HAzSSC12, (c) CNAzSSC12, and (d) 1-dodecanethiol SAMs (A) before and (B) after irradiation with UV light.

assuming an isotropic molecular orientation and an occupied area for the azobenzene moieties of 43.4 Å^2 (2 × 21.7 Å^2), we can calculate the absorbances for the large $\pi-\pi^*$ absorption bands at λ_{max} to be 0.022, 0.024, and 0.029 for the HAzSSC12, C6AzSSC12, and CNAzSSC12 SAMs,[25] respectively; these should be detectable by this reflection spectroscopy instrument. However, no peaks around λ_{max} were observed in the SAM spectra. Under such reflection spectroscopy measurement conditions as the probe light approaching in the normal direction to a substrate plane (5° to the incident angle), only the parallel component of the transition moment with the substrate should appear in the spectra. Therefore, the absence of a distinguishable peak around λ_{max} indicates that almost all of the azobenzene moieties orient in the normal direction against the substrate plane. A very small peak around 350−400 nm appears only in the CNAzSSC12 SAM spectrum, which may reflect a less-ordered structure for the cyanoazobenzene moieties. However, a distinct absorption band or shoulder around 250 nm is clearly seen in the C6AzSSC12 and HAzSSC12 SAMs. This band is ascribable to the transition moment parallel to a molecular short axis of the azobenzene moieties[24] and is visible even when the azobenzene moieties are aligned normal to the surface. The CNAzSSC12 SAM, unlike the C6AzSSC12 and HAzSSC12 SAMs, has no clear band at 250 nm, which can be attributed to the fewer number of molecules on the surface as suggested by the IR data concerning the molecular density of the film.

The UV irradiation of the azobenzene SAMs produced small changes in their spectral shapes, as shown in Figure 7B. This result does not mean that there is no photoisomerization by irradiation. The spectra of the SAMs with cis azobenzenes that have no characteristic strong absorption bands (Figure 6b) should be similar to those shown in Figure 7B. We cannot judge from these spectra whether the azobenzenes isomerize in the SAM.

Common peaks that appeared around 490 nm in these spectra are understood to be a derivation from a baseline correction (a bare gold plate has a severe flexion around 490 nm) because a similar peak is observed even in the 1-dodecanethiol SAM (Figure 7A, trace d).

3.3. Dynamic Contact-Angle Measurements. The contact-angle measurement is quite sensitive to a change in surface properties. It has actually been used for the investigation of the photoisomerization of azobenzene on surfaces.[7f,8c,26] Figure 8a−c shows dynamic contact angles of C6AzSSC12, HAzSSC12, and CNAzSSC12 SAM surfaces against water, respectively. As schematically drawn in Figure 8 (right), the sample plate was suspended vertically from a microbalance with a thin wire and was gradually dipped into the water (advancing) and withdrawn (receding) in two cycles. The upper part of the plate was irradiated with vis light after UV light, and the middle part of the plate was irradiated with UV light in advance. The lower part was not irradiated with any light. The dynamic contact angles were recorded against a contact-line position.

The advancing angles (θ_{adv}) of C6AzSSC12 were 107−109° without photoirradiation (at the contact-line position from 0 to 7 mm), which is quite similar to the value of the corresponding azobenzenethiol (C6AzSH) SAMs.[3a] However, the receding angle (θ_{re}) was 93−95°at the same position, which is slightly lower than the value for C6AzSH (∼97°). [3a] As shown in the Figure, UV light irradiation resulted in a decrease in contact angles whereas vis light irradiation helped the contact angles to recover almost to their original values. The changes in the contact angles by photoirradiation were $\Delta\theta = 4-5°$ for both the advancing and receding angles.

The HAzSSC12 SAM exhibited advancing angles (θ_{adv}) of 94−96° and a receding angle (θ_{re}) of 73−75° at the surface without photoirradiation. These values are reasonable when compared to those of aromatic surfaces ($\theta_{adv} = 92-98°$),[27] suggesting that the azobenzene moiety of HAzSSC12 having no substituent at the para position can directly interact with water on the surface. However, the hysteresis of the HAzSSC12 SAM is relatively large ($\Delta\theta_{adv-re} = 21°$) compared with that of the corresponding azobenzene-terminated SAM ($\Delta\theta_{adv-re} = 10°$),[3d] reflecting the surface inhomogeneity on the SAM introduced by asymmetrical disulfide structures (a mixture of aromatic terminals with methyl terminals). The HAzSSC12 SAM exhibited a similar photoresponse to that of the C6AzC12SSC12 SAM—a decrease in the contact angle on UV irradiation and a recovery on vis irradiation. The difference between the UV-irradiation region and the non- or vis-irradiation region was $\Delta\theta = 5-7°$, which was slightly greater than that of the C6AzSSC12 sample.

The CNAzSSC12 SAM exhibited advancing angles (θ_{adv}) of 79−81° and a receding angle (θ_{re}) of 47−48°. These values are definitely greater than the value of the CN-terminated surface in the previous report ($\theta_{adv} = 60$ or 63°).[28] The data suggest that there is a difference in the electronic state of the cyano group by conjugation with a phenyl ring or by the influence of the hydrophobic dodecyl chains mixed with the surface cyano groups. The large hysteresis ($\Delta\theta_{adv-re} = 32°$) of a CNAzSSC12 SAM between the advancing and receding angle might be interpreted by the molecularly disordered structure of the CNAzSSC12 SAM, as indicated by the IR-RA and UV spectra. On a disordered surface, the molecular orientations can be easily changed by the stress applied by the surface tension of the contacting water, which results in the large hysteresis of the contact angles. In contrast to the C6AzSSC12 and HAzSSC12 SAMs, the irradiation of a CNAzSSC12 SAM leads to only a slight shift in the contact angle, where the receding angles were increased by UV irradiation; however, the advancing angles were somewhat decreased by the same condition. This weak and opposite response in θ_{adv} and θ_{re} might be interpreted by the disordered film structure as well, where the mobility of the molecular tails possibly makes the photoresponse on the SAM unclear and irregular. Since a large effect due to the conformational change in the molecules by wetting and dewetting is unavoidable, it is difficult to conduct a qualitative analysis of the contact angles for such a disordered surface.

3.4. Calculation of Dipole Moments of Model Compounds. It is known that the physical properties of azobenzene are changed with photoisomerization. For example, the dipole moments of azobenzene isomers are quite different.[29] We estimated the values of the 4-hexyl- and 4-cyano-4′-butoxyazobenzenes as model compounds for the azobenzene moieties

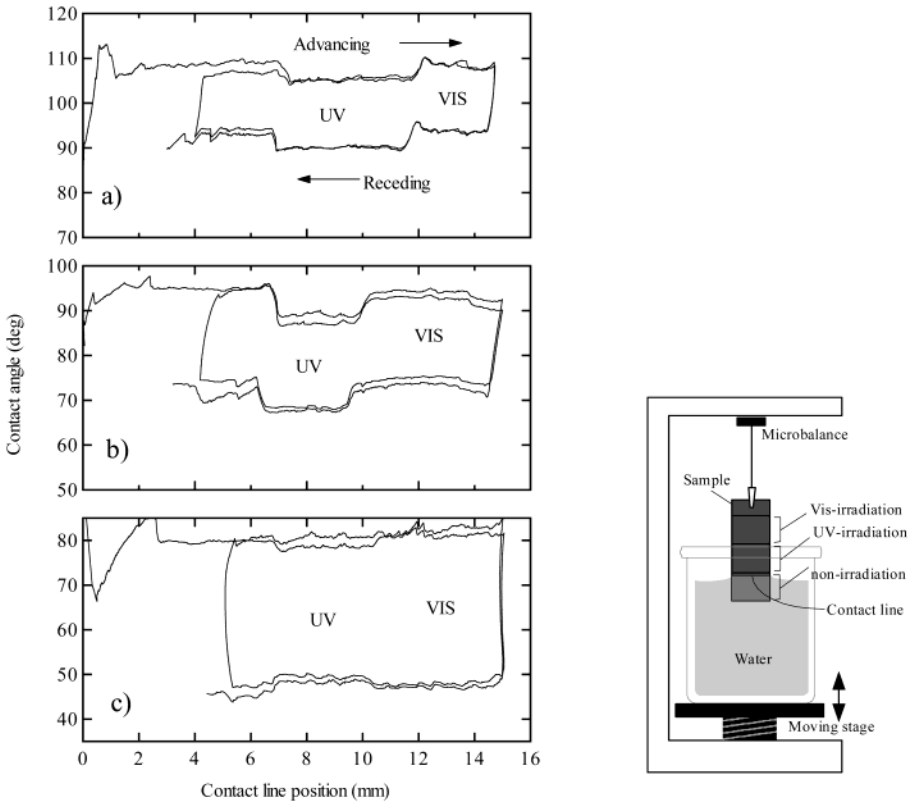

Figure 8. Dynamic contact angles of (a) C6AzSSC12, (b) HAzSSC12, and (c) CNAzSSC12 SAMs vs water and the schematic of the experimental setup (right).

of the disulfides by using molecular mechanics and MOPAC (AM1). As a result, the trans and cis forms of 4-butoxy-4′-hexyazobenzenes had dipole moments of 1.21 and 4.92 D, respectively. The increase in the dipole moment of the cis form is due to an asymmetric bent structure and the electron-withdrawing properties of an azo unit (N═N). From this calculation result, we can expect the polar cis isomer to produce low contact angles due to the dipole−dipole interaction with water that is larger than that of the trans isomer. As shown in Figure 8a, the contact angles of the C6AzSSC12 SAM are decreased by UV light irradiation and increased by vis light irradiation in agreement with this consideration. The trans isomer of 4-cyano-4′-butoxyazobenzene has a dipole moment of 4.93 D due to the strongly electron-withdrawing cyano group, but the dipole moment of the cis isomer is only 2.77 D because the electron-withdrawing properties of the cyano group and the azo group were partially canceled out. The small dipole moment of *cis*-cyanoazobenzene would account for the results of a slightly higher receding contact angle on UV irradiation as the result of a lower dipole−dipole interaction with water. However, a slightly lower advancing angle on this surface by UV irradiation cannot be explained by the same concept. The disordered and loosely packed structures are considerable for this case. This disordered structure apparently originates in the large dipole moment of *trans*-cyanoazobenzene, where the repulsive dipole−dipole interaction between cyanoazobenzene molecules can prevent the parallel alignment of the CNAzSSC12 molecules and result in the disordered SAM structures as an equilibrium.[14a]

4. Conclusions

The IR-RA spectra indicate relatively ordered structures in the methylene parts for the C6AzSSC12 and HAzSSC12 SAMs, but these SAMs show a photoresponse that is seen in the dynamic contact-angle measurement, indicating that there are

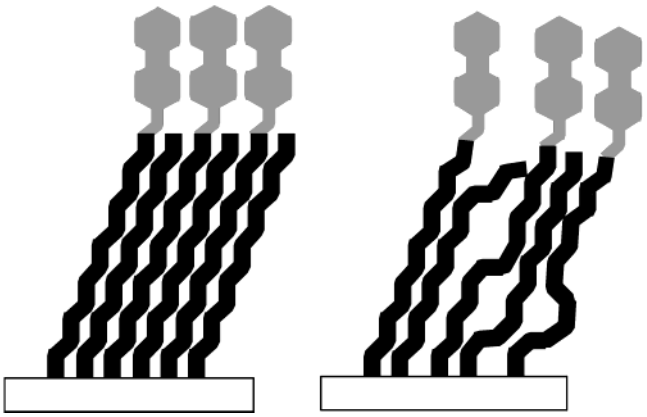

Figure 9. Schematic representations of the structures of C6AzSSC12 and HAzSSC12 SAMs (left) and the structure of a CNAzSSC12 SAM-(right).

free spaces for isomerization around azobenzene moieties. To increase the stability of the SAM, an ordered and packed structure is needed, whereas the free space is necessary to achieve a repeatable molecular transformation due to photoisomerization. The SAM composed of an asymmetric disulfide filled this contradictory requirement. However, the CNAzSSC12 SAM has a less-ordered SAM structure, as seen in the IR-RA spectra, and its photoresponse is rather unstable. This fact indicates that the substituent of the azobenzene moieties is also an important factor in regulating the photoreactivity as well as the SAM structures. For the case of the CNAzSSC12 SAM, a repulsive interaction between the large dipole moments in the cyanoazobenzene moieties significantly affected the SAM formation process and structures. Considering the results of the UV absorption spectra, which revealed that the long axis of all of the azobenzene units was oriented almost normal to the surface, we illustrate the schematic structure of the asymmetric

azobenzene SAMs as shown in Figure 9. Although the structure and photoreactivity of the SAMs are dependent on the substituents at the para position of the azobenzene moieties, the asymmetric disulfide SAM is useful for the application to potential photofunctions that require a conformational change in the uppermost SAM surfaces.

Acknowledgment. We thank Dr. R. Azumi of AIST for her kind help with the IR-RA spectroscopy.

References and Notes

(1) (a) Nuzzo, R. G.; Fusco, F. A.; Allara, D. L. *J. Am. Chem. Soc.* **1987**, *109*, 2358. (b) Brain, C. D.; Troughton, E. B.; Evall, Y. T.; Whitesides, G. M. *J. Am. Chem. Soc.* **1989**, *111*, 321. (c) Porter, M. D.; Bright, T. B.; Allara, D. L.; Chidsey, C. E. D. *J. Am. Chem. Soc.* **1987**, *109*, 3559.

(2) Laibinis, P. E.; Palmer, B. J.; Lee, S.-W.; Jennings, G. K. In *Self-Assembled Monolayers of Thiols;* Ulman, A.; Ed.; Thin Films; Academic Press: San Diego, CA, 1998; Vol. 24, Chapter 1.4.

(3) (a) Tamada, K.; Nagasawa, J.; Nakanishi, F.; Abe, K.; Ishida, T.; Hara, M.; Knoll, W. *Langmuir* **1998**, *14*, 3264. (b) Caldwell, W. B.; Campbell, D. J.; Chen, K.; Herr, B. R.; Mirkin, C. A.; Malik, A.; Durbin, M. K.; Dutta, P.; Huang, K. G. *J. Am. Chem. Soc.* **1995**, *117*, 6071. (c) Jaschke, M.; Schönherr, H.; Wolf, H.; Butt, H.-J.; Bamberg, E.; Besocke, M. K.; Ringsdorf, H. *J. Phys. Chem.* **1996**, *100*, 2290−2301. (d) Wolf, H.; Ringsdorf, H.; Delamarche, E.; Takami, T.; Kang, H.; Michel, B.; Gerber, Ch.; Jackschke, M.; Butt, H.-J.; Bamberge, E. *J. Phys. Chem.* **1995**, *99*, 7102.

(4) Wang, R.; Yoda, T.; Jiang, L.; Tryk, D. A.; Hashimoto, K.; Fujishima, A. *J. Electroanal. Chem.* **1997**, *438*, 213.

(5) Vector, J. G.; Torkelson, J. M. *Macromolecules* **1987**, *20*, 2241.

(6) (a) Iwamoto, M.; Kanai, Y.; Naruse, H. *J. Appl. Phys.* **1993**, *74* 1131. (b) Seki, T.; Ichimura, K. *Thin Solid Films* **1989** *179*, 77. (c) Xu, X. B.; Majima, Y.; Iwamoto, M. *Thin Solid Films* **1998**, *331*, 239. (d) Weener, J.-W.; Meijer, E. W. *Adv. Mater.* **2000**, *12*, 741.

(7) (a) Sekkat, Z.; Wood, J.; Geerts, Y.; Knoll, W. *Langmuir* **1996**, *12*, 2976. (b) Xing, L.; Mattice, W. L. *Langmuir* **1996**, *12*, 3024. (c) Mouanda, B.; Viel, P.; Blanche, C. *Thin Solid Films* **1998**, *323*, 42. (d) Aoki K.; Hosoki, A.; Ichimura, K. *Langmuir* **1992**, *8*, 1007. (e) Ichimura, K.; Suzuki, Y.; Hosoki, A.; Aoki K. *Langmuir* **1988**, *4*, 1214. (f) Siewierski, L. M.; Brittain, W. J.; Petrash, S.; Foster, M. D. *Langmuir* **1996**, *12*, 5838.

(8) (a) Ichimura, K.; Fukushima, N.; Fujimaki, M.; Kawahara, S.; Matsuzawa, Y.; Hayashi, Y.; Kudo, K. *Langmuir* **1997**, *13*, 6780. (b) Fujimaki, M.; Kawahara, S.; Matsuzawa, Y.; Kurita, E.; Hayashi, Y.; Ichimura, K. *Langmuir* **1998**, *14*, 4495. (c) Oh, S.; Nakagawa, M.; Ichimura, K. *Chem. Lett.* **1999**, 349.

(9) Nakagawa, M.; Watase, R.; Ichimura, K. *Chem. Lett.* **1999**, 1209.

(10) (a) Liu, G. Y.; Salmeron, M. B. *Langmuir* **1994**, *10*, 367. (b) Li, T. T. T.; Weaver, M. J. *J. Am. Chem. Soc.* **1984**, *106*, 6107.

(11) Evans, S. D.; Johnson, S. R.; Ringsdorf, H.; Williams, L. M.; Wolf, H. *Langmuir* **1998**, *14*, 6436.

(12) (a) Bain, C. D.; Whitesides, G. M. *J. Am. Chem. Soc.* **1989**, *111*, 7164. (b) Tamada, K.; Hara, M.; Sasabe, H.; Knoll, W. *Langmuir* **1997**, *13*, 1558.

(13) (a) Noh, J.; Hara, M. *Langmuir* **2000**, *16*, 2045. (b) Heister, K.; Allara, D. L.; Bahnck, K.; Frey, S.; Zharnikov, M.; Grunze, M. *Langmuir* **1999**, *15*, 5440.

(14) (a) Ishida, T.; Yamamoto, S.; Mizutani, W.; Motomatsu, M.; Tokumoto, H.; Hokari, H.; Azehara, H.; Fujihira, M. *Langmuir* **1997**, *13*, 3261. (b) Ishida, T.; Yamamoto, S.; Motomatsu, M.; Mizutani, W.; Tokumoto, H.; Hokari, H.; Azehara, H.; Fujihira, M.; Kojima, I. *Jpn. J. Appl. Phys.* **1997**, *36*, 3909.

(15) (a) Chen, S.; Li, L.; Boozer, C. L.; Jiang, S. *J. Phys. Chem. B* **2001,** *105*, 2975. (b) Shon, Y.-S.; Mazzitelli, C.; Murry, R. W. *Langmuir* **2001**, *17*, 7735.

(16) Akiyama, H.; Tamada, K.; Nagasawa, J.; Nakanishi, F.; Tamaki, T. *Trans. Mater. Res. Soc. Jpn.* **2000**, *25*, 425.

(17) (a) Tamada, K.; Akiyama, H.; Wei, T. X. *Langmuir* **2002**, *18*, 5239. (b) Tamada, K.; Akiyama, H.; Wei, T. X.; Kim. S.-A. *Langmuir*, submitted for publication.

(18) Newman, A. W.; Good, R. J. In *Surface and Colloid Science;* Good, R. J., Stromberg, R. R., Eds.; Plenum Press: New York, 1979; Vol. 11, Chapter 2.1.2.

(19) Takiguchi, H.; Sato, K.; Ishida, T.; Abe, K.; Yase, K.; Tamada, K. *Langmuir* **2000**, *16*, 1703.

(20) (a) Biswas, N.; Umapathy, S. *J. Phys. Chem. A* **1997**, *101*, 5555. (b) Nakahara, H.; Fukuda, K. *J. Colloid Interface Sci.* **1983**, *93*, 530. (c) Zhang, H. L.; Zhang, J.; Li, H. Y.; Liu, Z. F.; Li, H. L. *Mater. Sci. Eng., C* **1999**, *8/9*, 179. (d) Meic, Z.; Baranovic, G.; Smercki, V.; Novak, P.; Keresztury, G.; Holly, S. *J. Mol. Struct.* **1997**, *408/409*, 399.

(21) Ihs, A.; Uvdal, K.; Liedberg, B. *Langmuir* **1993**, *9*, 739.

(22) Wu, Y.; Zhao, B.; Xu, W.; Li, B.; Jung, Y. M.; Ozaki, Y. *Langmuir* **1999**, *15*, 4625.

(23) It is known that the carbon number of the methylene parts in the ordered alkanethiol−Au SAM strongly affects the orientational direction of the uppermost CH_3 group. Colorado, R.; Villazana, R. J.; Lee, T. R. *Langmuir* **1998**, *14*, 6337.

(24) (a) *Light Absorption of Organic Colorants*; Fabian, J., Hartmann, H., Eds.; Springer-Verlag: Berlin, 1980; Chapter 7. (b) Robin, M. B.; Shimpson, W. T. *J Chem. Phys.* **1962**, *36*, 580. (c) Uznanski, P.; Kryszewsky, M.; Thuulstrup, E. W. *Spectrochim. Acta, Part A* **1990**, *46*, 23.

(25) $\mathrm{abs(SAM)} = 2\epsilon cl = 2\epsilon \times 1000/43.4/(10^{-8})^2/6.02/10^{23}$, where abs, ϵ, c, and l are the absorbance, molar extinction coefficient ($\mathrm{mol^{-1}\ L\ cm^{-1}}$), concentration (mol/L), and length (cm).

(26) Ishihara, K.; Hamada, N.; Kato, S.; Shinohara, I. *J. Polym. Sci.* **1983**, *21*, 1551.

(27) (a) Lee, S.; Puck, A.; Graupe, M.; Colorado, R.; Shon, Y. S.; Lee, T. R.; Perry, S. S. *Langmuir* **2001**, *17*, 7364. (b) Filippini, P.; Rainaldi, C.; Ferrante, A.; Mecheri, B.; Gabrielli, G.; Bombace, M.; Indovina, Pl.; Santini, M. T. *J. Biomed. Mater. Res.* **2001**, *55*, 338. (c) Zangmeister, R. A. P.; Smolenyak, P. E.; Drager, A. S.; O'Brien, D. F.; Armstrong N. R. *Langmuir* **2001,** *17*, 7071. (d) Choi, N.; Ishida, T.; Inoue, A.; Mizutani, W.; Tokumoto, H. *Appl. Surf. Sci.* **1999**, *144−145*, 445.

(28) (a) Cidsey, C. E. D.; Loiacono, D. N. *Langmuir* **1990**, *6*, 682 (60° as advancing). (b) Bain, C. D.; Whitesides, G. M. *Angew. Chem., Int. Ed. Engl.* **1989**, *28*, 506 (63° as advancing).

(29) Delang, J. J.; Robertson, J. M.; Woodward, I. *Proc. R. Soc. London, Ser. A* **1939**, *171*, 398.